Journal of Polymers and the Environment (2022) 30:5290–5300
https://doi.org/10.1007/s10924-022-02619-7

ORIGINAL PAPER

Exploring Potential of Adsorptive-Photocatalytic Molybdenum Disulphide/Polyacrylonitrile (MoS_2/PAN) Nanofiber Coated Cellulose Acetate (CA) Membranes for Treatment of Wastewater

Nur Shafiqah Jamaluddin[1] · Nur Hashimah Alias[1] · Juhana Jaafar[2] · Nur Hidayati Othman[1] · Samitsu Sadaki[3] · Fauziah Marpani[1] · Woei Jye Lau[2] · Mohd Haiqal Abd Aziz[4]

Accepted: 27 September 2022 / Published online: 13 October 2022

Abstract

Adsorptive-photocatalytic electrospun nanofiber membranes have received remarkable attention as they could provide an excellent solution for the effective treatment of wastewater. However, the mechanical properties of nanofiber have limited their use in pressure-driven filtration applications. In this study, dual-layered MoS_2/PAN-CA adsorptive-photocatalytic-based membranes have been successfully fabricated using molybdenum disulphide/polyacrylonitrile (MoS_2/PAN) nanofiber coated porous cellulose acetate (CA) membranes. The fabricated CA membranes were coated with electrospun MoS_2/PAN nanofiber via the electrospinning technique. Subsequently, hot-pressed treatment was applied to the fabricated membrane to form a stronger attachment between the CA and MoS_2/PAN nanofiber layers. The physicochemical properties of the fabricated membranes were characterised using scanning electron microscopy (SEM), energy dispersive X-ray (EDX), Fourier transform infrared spectroscopy (FTIR), thermogravimetric analyzer (TGA), water contact angle (WAC), porosity analysis, and tensile strength test. In addition, the membrane separation performance of the fabricated nanofiber membranes was evaluated in terms of water flux and contaminant rejection using a self-assembled cross-flow filtration system. The MoS_2/PAN-CA membrane demonstrated improved physicochemical and structural properties where WAC, porosity and mechanical strength increased up to 38% (44.0°), 25% (55%) and 26% (32.1 MPa), respectively, as compared to pristine CA membrane. Upon hot-pressed treatment at a temperature of 120 °C, pure water flux of MoS_2/PAN-CA membrane improved by 28% to 36.3 $Lm^{-2}\,h^{-1}$. These improved properties of dual-layered adsorptive-photocatalytic MoS_2/PAN-CA membranes recommend it as a potential membrane material to treat various pollutants in water and wastewater.

Keywords Electrospinning · MoS_2 · Adsorptive · Membrane · Pure water flux · Cellulose acetate

✉ Nur Hashimah Alias
nurhashimah@uitm.edu.my

[1] Department of Oil and Gas Engineering, School of Chemical Engineering, College of Engineering, Universiti Teknologi MARA, 40450 Shah Alam, Selangor, Malaysia

[2] Advanced Membrane Technology Research Centre (AMTEC), School of Chemical and Energy Engineering, Faculty of Engineering, Universiti Teknologi Malaysia, 81310 Skudai, Johor, Malaysia

[3] Research and Services Division of Materials Data and Integrated System (MaDIS), National Institute for Materials Science, 1-2-1, Sengen, Tsukuba 305-0047, Japan

[4] Department of Chemical Engineering Technology, Faculty of Engineering Technology, Universiti Tun Hussein Onn Malaysia, Pagoh Higher Education Hub Muar, 84600 Batu Pahat, Johor, Malaysia

Introduction

Water pollution by organic pollutants has become a severe worldwide concern as it causes many harmful effects on the aquatic ecosystem and human health. The most typical organic pollutants in water and wastewater effluent are organic dyes and pesticides [1]. With the increase in industrial activities which contribute to the destruction of water resources, it becomes urgent to develop an efficient treatment to eliminate organic pollutants. Numerous treatment strategies have been applied, including ion exchange, electrochemical reduction, chemical precipitation, adsorption and photocatalytic degradation. Among these approaches, photocatalytic degradation is the most effective method to remove a wide range of organic pollutants [2–4]. However, additional separation processes like centrifugation are often

required for the method to completely remove photocatalyst from the whole system after the process is completed [5].

Membrane separation technology provides a one-step treatment procedure, and it has been considered a new promising alternative for removing organic contaminants due to its convenient and cost-effective process [6–8]. On top of that, nanofiber membranes have received myriad attention for application in wastewater treatment due to their unique properties such as large specific surface area, interconnected pores, flexibility and high porosity [9]. Electrospinning has emerged as the most versatile technique to produce nanofiber with controllable diameters from nanometers to several micrometres [9, 10]. Due to its unique properties, electrospun nanofiber membrane (ENM) has been massively used for photocatalyst interphase to regenerate the spent photocatalysts, hence overcoming the photocatalytic process's limitation [11]. Polyacrylonitrile (PAN) polymer is one of the most common synthetic polymers used as a photocatalytic substrate during electrospinning [12]. PAN was categorized under non-toxic synthetic polymer, which has low cost and provides excellent thermal stability, solvent resistance, environmental stability, and small interfibrous pore size [5, 13]. Moreover, PAN has high UV light resistance, which is applicable in photocatalytic degradation [14].

Recently, molybdenum disulfide (MoS_2) photocatalysts have received widespread attention in organic contaminants removal due to their high electron conductivity, large surface area, and rich active sites [15–17]. Furthermore, MoS_2 has a narrow bandgap of approximately 1.8 eV, making it a potential candidate for removing organic pollutants, especially under UV light irradiation [18]. Theoretically, the S-Mo-S layer structure of the MoS_2 sheet puts S exposed on the surface, which provides a high number of active sites for affinity adsorption [19, 20]. The negatively charged surface of MoS_2 could enhance the adsorption of organic pollutants that have positively charged ions. Several researchers have proven the effectiveness of MoS_2 embedded in a solid matrix substrate for the removal of organic contaminants, including methylene blue [21–23], rhodamine B [24], pyridine [25] and endocrine [26]. For instance, Zhao et al. [27] reported that the deposition of MoS_2 and polydopamine on ultrafiltration membranes could achieve 99% rejection of methylene blue [21]. Generally, immobilizing the photocatalytic nanofiber on membrane substrate by physical coating is one of the effective methods to enhance the membrane filtration performance and fouling issue of the membranes [28, 29]. However, the strength of attachment between these photocatalytic nanofiber layers and membrane substrate could be one of the significant concerns in the fabrication of this membrane.

Cellulose acetate (CA) is the most typical substrate used for membrane preparation due to its wide availability from natural sources, high chemical resistance, low cost and high thermal properties. [30–33]. However, many researchers indicated the performance of the CA membrane could be further improved by adding some additives and surface modifications like blending of polymers, chemical grafting and coating on the membrane surface [34]. Therefore, this study aims to enhance the mechanical strength of MoS_2/PAN nanofiber by coating the nanofiber layer on the CA membrane after hot-pressed treatment for water remediation since it has not yet been reported. Furthermore, hot-pressed treatment at different temperatures on the MoS_2/PAN nanofiber and CA membrane were also investigated and characterised.

Methodology

Materials

Cellulose acetate (CA, MW = 30 000 g/mol) and polyacrylonitrile (PAN, MW = 150,000 g/mol were used as polymer material to prepare composite membranes. Commercial molybdenum disulfide (MoS_2) powder with purity > 99% synthesised MoS_2 nanofiber. N, N-dimethylformamide (DMF, 99%), was selected as the solvent in preparing nanofibrous composite membranes. All the chemicals were purchased from Sigma Aldrich without further purification.

Fabrication of CA membranes

In this study, CA membranes were fabricated using the phase inversion technique. A 13 wt% of CA powder was dissolved in 87 wt% of DMF solvent at 27 °C up until 24 h to form a homogenous polymer dope solution. Before membrane casting, the prepared dope solution was degassed for 2 h in an ultrasonic bath to ensure no air bubbles in the solution. This is an important step to minimise structural defects on the membrane [35]. During the membrane casting process, the prepared dope solution was poured on a glass plate and immediately, by using a glass rod, the poured dope solution was spread uniformly to form a sheet layer of CA membrane. After 60 s, the glass plate was subsequently immersed in the water bath at 25 °C together to allow the solvent exchange of DMF and water. Lastly, the casted flat sheet CA membranes were dried overnight at room temperature.

Fabrication of nanofibers and nanofibers coated CA membranes

A 10 wt% PAN dope solution for the electrospinning process was prepared as the control, and in this study, nanofibers were fabricated using Nanofibers Electrospinning Unit (Progene Link Sdn. Bhd., NF-1000). First, MoS_2/PAN nanofibers were fabricated by preparing a dope solution containing a 1.9 wt% MoS_2 in DMF and PAN. Prior to that, MoS_2 was exfoliated in dispersing solvent, DMF and further sonicated

for 2 h. The dope solution was filled in a 10 mL plastic syringe and placed 18 cm from a ground collector with a rotating speed of 180 rpm during the electrospinning process. The ground collector was wrapped with aluminium foil to peel the electrospun nanofibers easily. The dope solution was electrospun under processing conditions of 15 kV voltage and a 1.0 ml/hr of dope solution flow rate using a 21G metallic needle. Then, the electrospinning process was conducted under room conditions. To coat CA membranes with nanofibers, a square CA membrane with a dimension of 15 cm × 15 cm was stuck on the ground collector and further electrospun directly onto the surface of the CA membrane. Lastly, the prepared PAN nanofibers coated CA membrane (PAN-CA membrane), and MoS_2/PAN nanofiber coated CA membrane (MoS_2/PAN-CA membrane) were dried for 24 h at room temperature. The electrospun PAN nanofiber and MoS_2/PAN nanofibers without CA membrane support were also fabricated using similar steps to characterise their properties. To improve the coating attachment of nanofiber on the CA membrane, a hot-pressed method according to a technique by [36] was applied (Fig. 1). The prepared PAN-CA membranes and MoS_2/PAN-CA membranes were hot-pressed for at least 180 s. During the hot-pressed process, two different temperatures were applied (90 °C and 120 °C) to ensure the best temperature for a good nanofiber coating onto the surface of the CA membrane. The schematic illustration for the complete process for the preparation of the MoS_2/PAN-CA membrane is shown in Fig. 2.

Characterization of fabricated nanofibers and membranes

The surface morphology of the fabricated membranes was observed using a scanning electron microscope (SEM) (Hitachi SU8020). The freeze-fracture method has been used to prepare cross-sections of membranes for visualization

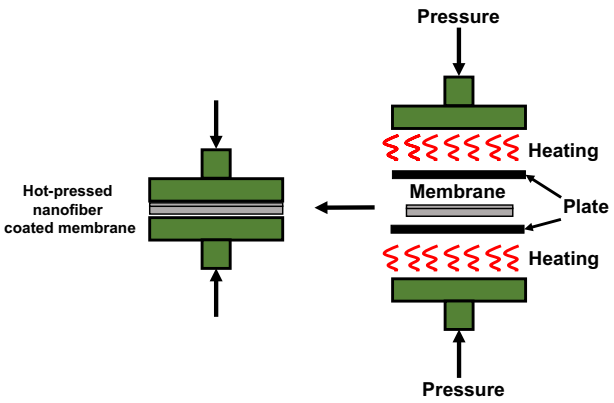

Fig. 1 Schematic diagram of hot-pressed method of nanofiber coated membrane

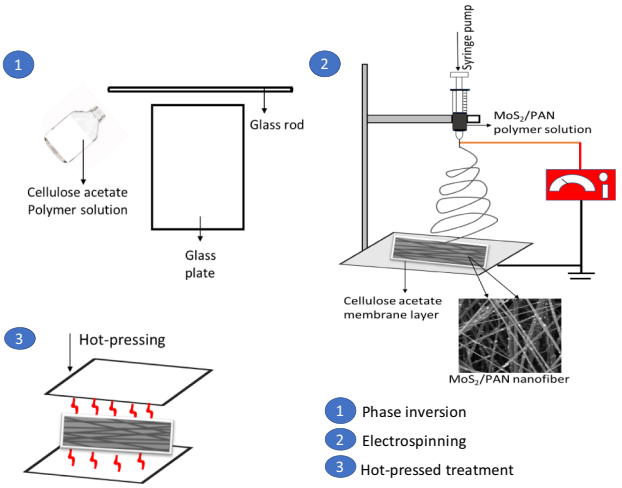

Fig. 2 Schematic illustration for preparation step for MoS_2/PAN-CA membrane via phase inversion and electrospinning with hot-pressed treatment

using SEM. The membrane samples were fractured by immersing in liquid nitrogen until the sample was completely frozen. After that, a sharp scalpel was then cooled in the bath and quickly used to cut the membranes in one step. Before scanning, the membranes were fixed with double-sided carbon tape and coated with a thin platinum layer. The elemental mappings of the prepared membranes were observed using an energy dispersive X-ray analyzer (EDX). Fourier transform infrared spectroscopy (FTIR, Perkin-Elmer, USA) was used to analyse the membranes' chemical structure, and the FTIR spectra were recorded at the wavenumber between 600 and 4000 cm. The thermal stability of the composite membrane was determined using a thermogravimetric analyzer (TGA4000, Perkin Elmer Inc.) under nitrogen gas at a heating rate of 10 °C/min to 800 °C. The dry–wet technique was employed to determine the porosity of membranes. The relative hydrophilicity of the prepared membrane was determined by the contact angle measurement. The contact angle was measured using the static sessile drop method with a goniometer (Model: OCA 15EC, Dataphysics), and deionized water was used as the liquid probe. The tensile strength of nanofiber and flat sheet membrane was evaluated by a material testing machine (H5K-S, UK) under a crosshead speed of 5.0 mm/min under room conditions. The tensile specimens were cut into strips 10 mm wide and 60 mm long, and the gap distance between the claws was fixed at 50 mm before the testing.

Water flux performance

The performance of the prepared membranes in terms of water flux was evaluated using a cross-flow filtration

setup, as shown in Fig. 3. A 47 mm diameter membrane was tested during the measurement using a 1000 ml distilled water as feed and transmembrane pressure of 1 bar for 1.5 h. To calculate its pure water flux permeability, the permeate was collected every 30 min. The collected permeate was recycled to the feed tank. The water flux was calculated using Eq. 1 [37].

$$W_f = \frac{V}{A\Delta t} \quad (1)$$

where W_f is the water flux ($L \cdot m^{-2} \cdot h^{-1}$), V is the volume (L) of the feed solution, A is the area (m^2) of the membrane, and t is the time (h).

Results and Discussion

Structural and physicochemical of the prepared nanofibers and membranes

The SEM images of PAN nanofiber and MoS_2/PAN nanofiber are shown in Fig. 4a–d, respectively. As shown in Figs. 4a and b, PAN nanofiber presents a straight, smooth and uniform distribution of fine nanofiber, which explains a proper and successful electrospinning process. On top of that, the nanofiber also displayed an overlapping nanofiber structure and formed interconnected pores [38]. Upon incorporating exfoliated MoS_2 into PAN nanofiber, the nanofiber structure is still maintained straight and smooth with a uniform distribution of exfoliated MoS_2 on the nanofiber surface.

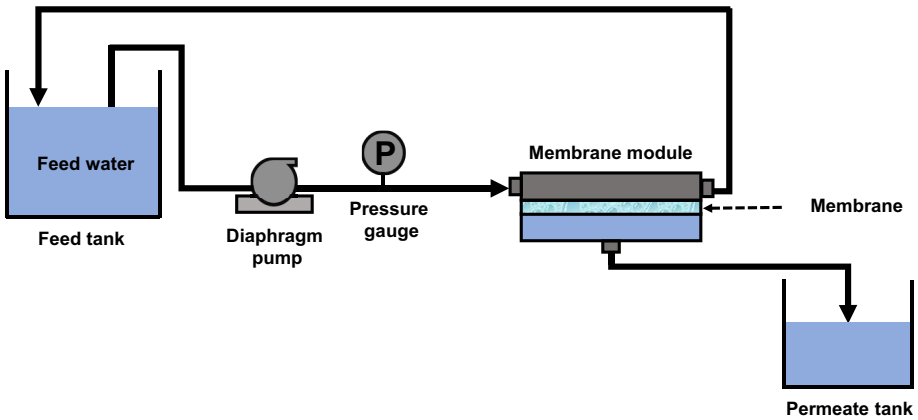

Fig. 3 Schematic diagram of the experimental setup for cross-flow filtration

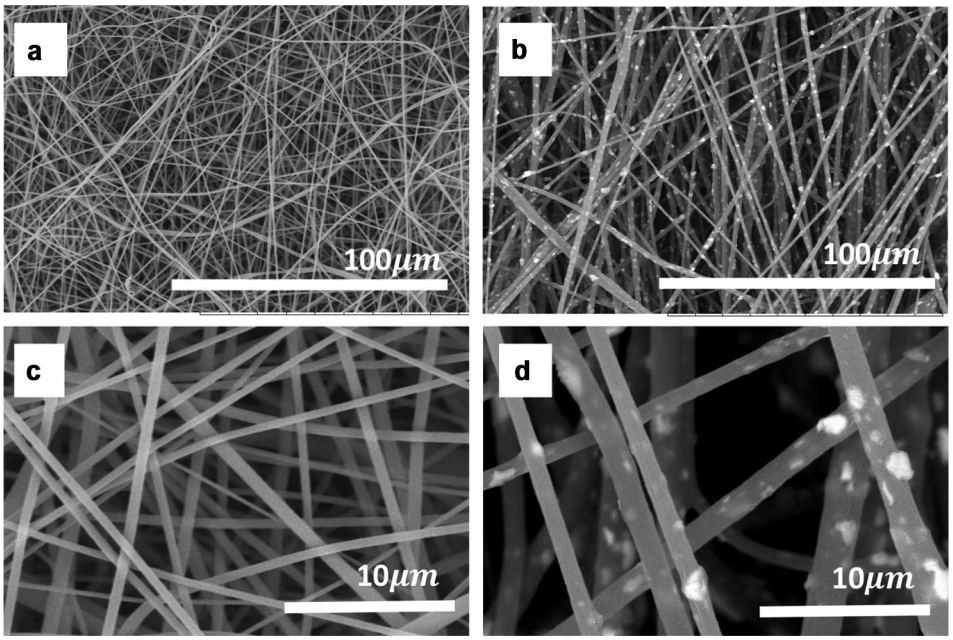

Fig. 4 SEM micrographs of (**a**) and (**b**) PAN nanofiber and (**c**) and (**d**) MoS_2/PAN nanofiber

Incorporation of 1.9 wt% exfoliated MoS_2 in PAN polymer dope solution successfully produced electrospun MoS_2/PAN nanofiber with uniform distribution of MoS_2, suggesting the compatibility of MoS_2 and PAN Figs. 4b–d. As a result, the diameter of nanofibers was drastically increased from 594 to 1020 nm as MoS_2 was beneath the PAN nanofiber surface. Besides that, the open pore size of MoS_2/PAN nanofiber also increased compared to pristine PAN nanofiber. A similar observation was reported in previous literature, mentioning that incorporating graphene oxide into PAN nanofiber via electrospinning resulted in increased fiber diameter from 475 ± 53 to 1356 ± 267 nm [39]. Moreover, a study by Rad et al., [40] also mentioned that the loading of zeolite nanomaterials also significantly changed the diameter of electrospun PVA nanofibers. The enlargement of nanofiber size was due to the changes in polymer solutions' electrical conductivity and viscosity attributed to the more powerful jet stretching [13].

Figures 5a and b show surface and cross-section SEM images of the prepared membrane samples. The images demonstrated that the CA membrane had scattered macropores on the membrane surface and macrovoids approximately ~ 50 µm in size. This finding also agrees with the previous study reported by Pandele et al., [41], that fabricated CA membrane via phase inversion technique and the resulted membrane has a thin porous skin layer at the top

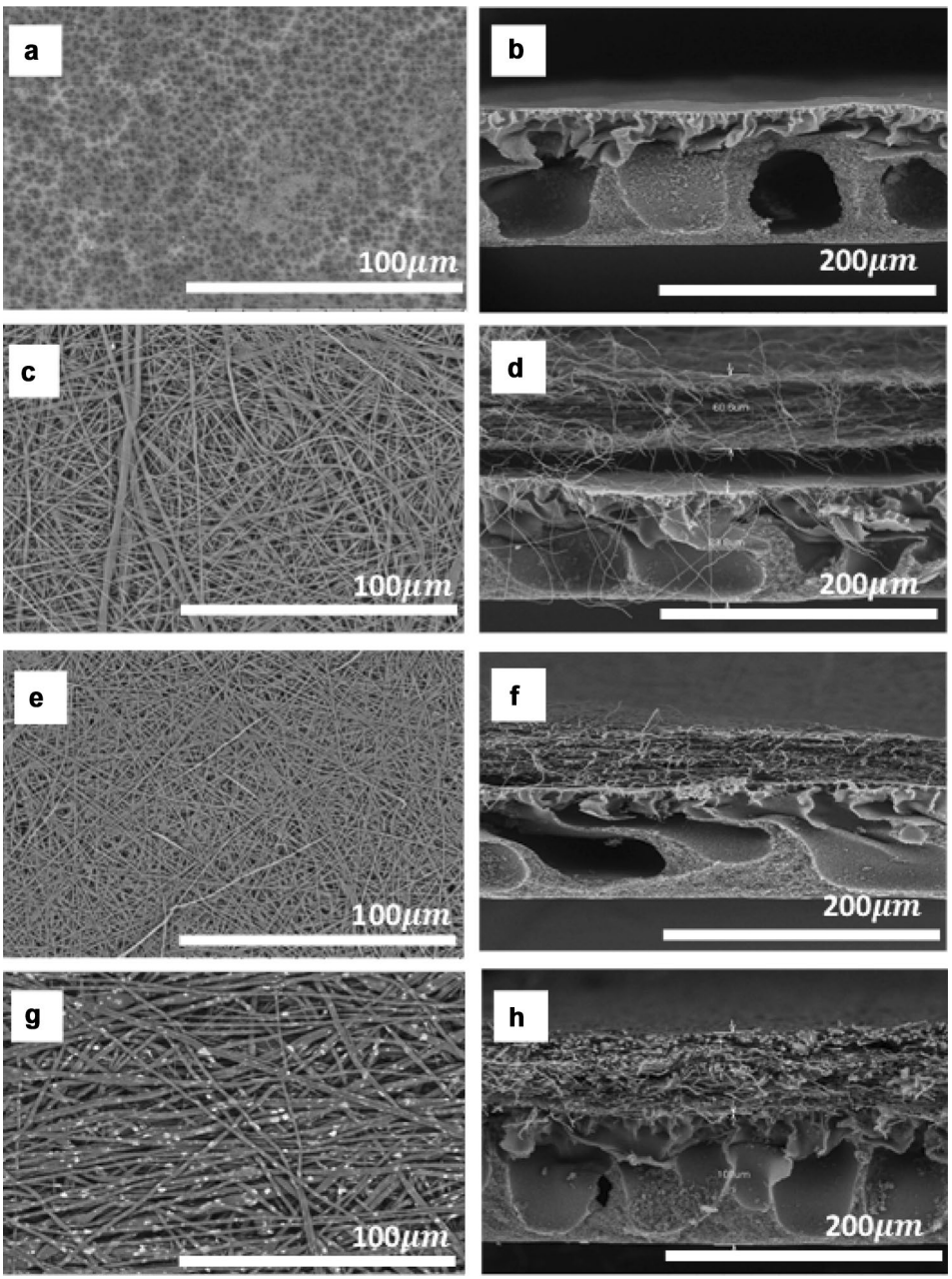

Fig. 5 Surface and cross-section SEM micrographs of (**a**) and (**b**) CA membrane, (**c**) and (**d**), PAN-CA@90 membrane, (**e**) and (**f**) PAN-CA membrane, (g) and (h) MoS_2/PAN-CA@120 membrane

surface and porous cross-section with some macrovoids. On the other hand, Figs. 5c and d shows the morphology of the fabricated PAN-CA@90 membrane. Upon hot-pressed at 90 °C, the roughness of PAN nanofiber was reduced without any substantial deformations. However, the cross-section of the fabricated membrane presented an empty layer between the CA membrane and PAN nanofiber, which demonstrates poor attachment with these layers.

On the contrary, as the hot-pressed temperature was increased to 120 ℃, the fabricated PAN-CA@120 membrane displayed a firm attachment between the nanofiber and membrane substrate (Figs. 5e and f). A good attachment between these two layers is vital to prevent the detachment of nanofiber during filtration operation. Therefore, to improve the membrane properties of the dual-layered MoS_2/PAN-CA membrane, hot-pressed treatment at a temperature of 120 ℃ was applied, and the SEM images of the fabricated membrane are shown in the Figs. 5g and h. Overall, the nanofibers remained straight and uniformed upon the addition of MoS_2 and hot-press treatment, indicating the nanofibers have a good attachment with the CA membrane without damaging their structural properties. Furthermore, the images confirmed the incorporation of MoS_2 in the PAN nanofiber as the MoS_2 photocatalyst was seen scattered on the fibers. The existence of MoS_2 was also confirmed by the results of EDX in Fig. 6. The synthesized MoS_2/PAN-CA membrane surface displayed the content of carbon, C (48.6 wt%), nitrogen, N (11.7 wt%), molybdenum, Mo (23.4 wt%) and Sulphur, S (16.3 wt%). Mo and S have represented the elements in MoS_2, whereas the high percentage of C and N probably are from PAN polymers. FTIR analysis was further conducted to verify the functional groups of the MoS_2/PAN-CA membrane.

Figure 7 shows the FTIR spectrum PAN nanofiber, MoS_2/PAN nanofiber, CA membrane, and MoS_2/PAN-CA membrane. The FTIR spectra of PAN nanofibers showed

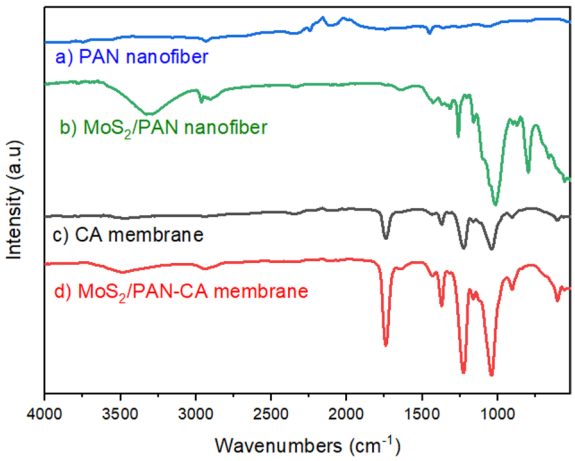

Fig. 7 FTIR spectrum of (**a**) PAN nanofiber, (**b**) MoS_2/PAN nanofiber, (**c**) CA membrane, and (**d**) MoS_2/PAN-CA membrane

strong absorption bands at 2245 cm^{-1} and 1445 cm^{-1}, corresponding to the stretching vibrations of −C≡N and N−H groups [42]. Meanwhile, the composite MoS_2/PAN nanofibers presented a characteristics band at 3327 cm^{-1} after incorporation of MoS_2, which is in agreement with previously reported data on MoS_2 [43]. The adsorption peaks of the CA membrane were generally observed in the region of 1734 cm^{-1} and near 3518 cm^{-1}, corresponding to the stretching of C=O bonds [44] and intermolecular hydrogen bonds of hydroxyl groups (− OH) [45]. In addition, a slight shift in the absorption peak of OH groups were observed in the FTIR spectra of the MoS_2/PAN-CA membrane. Thus, these peak characteristics proved the combination peaks of MoS_2/PAN nanofiber and CA membrane.

The thermal analysis profile in Fig. 8 provides information on the decomposition temperature of CA and MoS_2/PAN-CA membranes. Based on the TGA profiles, the thermal degradation of CA membrane without a coating layer

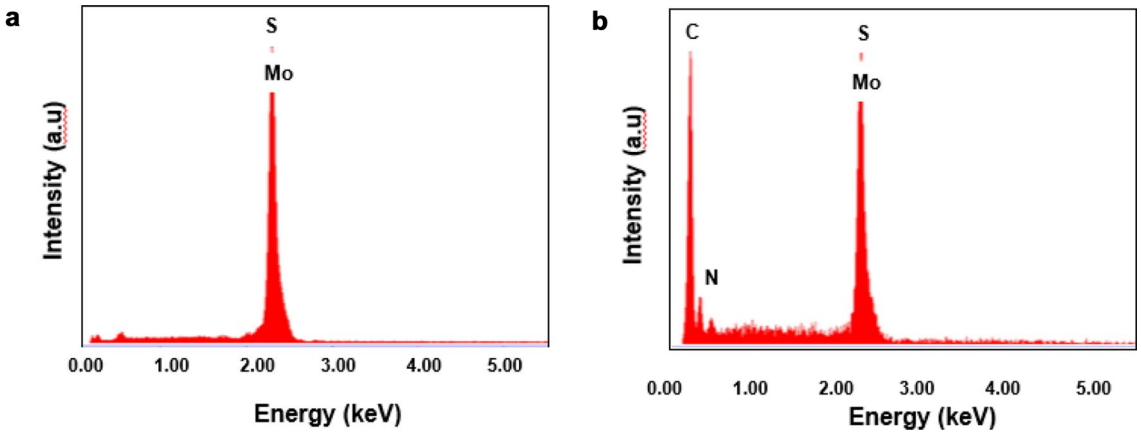

Fig. 6 EDX spectrum of (**a**) MoS_2 powder (**b**) MoS_2/PAN-CA membrane

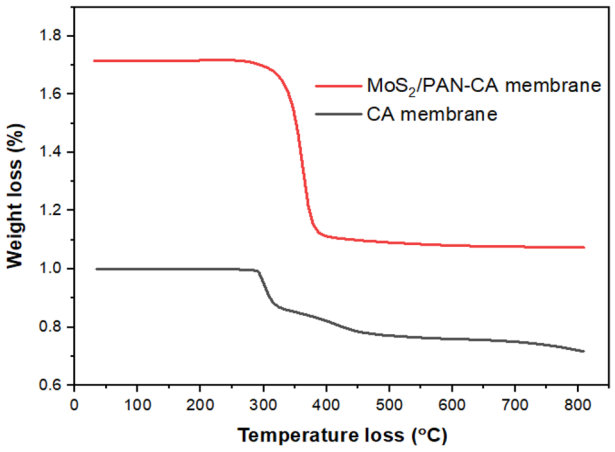

Fig. 8 TGA profile of MoS_2/PAN nanofiber and CA membrane

occurs approximately at 290 °C. The value is almost similar to the previously reported study by Lucena et al. [46]. The addition of MoS_2/PAN nanofiber coated on the CA membrane using the hot-pressed technique resulted in increased thermal degradation of the membrane. Furthermore, the weight loss on MoS_2/PAN-CA membrane was also found to be 0.2—0.3% lower than the CA membrane. Therefore, thermal stability enhancement is related to MoS_2/PAN nanofiber coating on CA membranes.

Water contact angles (WAC) for the fabricated membranes are presented in Fig. 9. First off, the contact angle of the CA membrane was observed at 70.8 °, indicating the hydrophilicity properties of the asymmetric CA membrane fabricated from the phase inversion method. On the contrary, PAN nanofiber demonstrated slight hydrophobic properties with the contact angle observed at 126.2° due to the overlapped layers of nanofiber [47] and the rough surface of nanofibers [37, 48] that resulted in a low contact area between nanofiber and water. On top of that, the addition of the MoS_2 in PAN nanofiber has increased the contact angle of MoS_2/PAN nanofiber.

Nevertheless, upon nanofiber coating on top of the CA membrane followed by hot-press treatment, the contact angles for both PAN-CA membrane and MoS_2/PAN-CA membrane reduced significantly and caused the membranes to have hydrophilic properties. It was plausibly due to the dense structure of the membrane after hot-press treatment [49]. Shahidul et al., [50] previously reported a similar result that hot-pressed membrane exhibited high hydrophilicity. However, MoS_2/PAN-CA membrane has a slightly higher contact angle than the PAN-CA membrane due to the pore blockage phenomenon by MoS_2, which is favourable for filtration of micropollutants. Nor et al. [36], previously mentioned that the hot-pressed TiO_2 nanofiber and PVDF membrane have caused the TiO_2 nanofiber to merge and aggregate with the PVDF matrices, resulting in a decreased hydrophilicity.

Membrane Porosity

Figure 10 shows the porosity (%) for the prepared nanofibers and membranes. PAN nanofiber and MoS_2 nanofiber demonstrated a higher percentage of porosity at 84% and 70%, respectively, compared to pristine CA membrane (30%) due to the mesh structure of the nanofibers. However, the porosity of the hot-pressed nanofibers coated CA membrane was found lower at 58% (PAN-CA membrane) and 55% (MoS_2/PAN-CA membrane), respectively. These porosities were reduced due to compression and collapse of membrane pores induced by pressure and temperature from hot-pressed and subsequently reduced the membrane porosity [51]. Furthermore, a hot-pressed technique enhanced the adherence of MoS_2/PAN nanofibers to the CA membrane, resulting in low porosity and smaller pore size distribution. The smaller

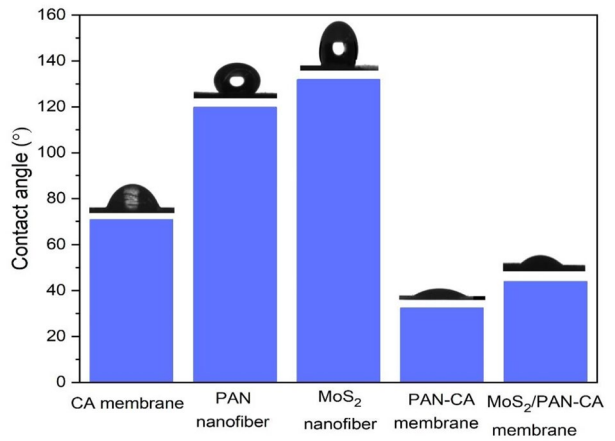

Fig. 9 Contact angle analysis on different types of fabricated membranes

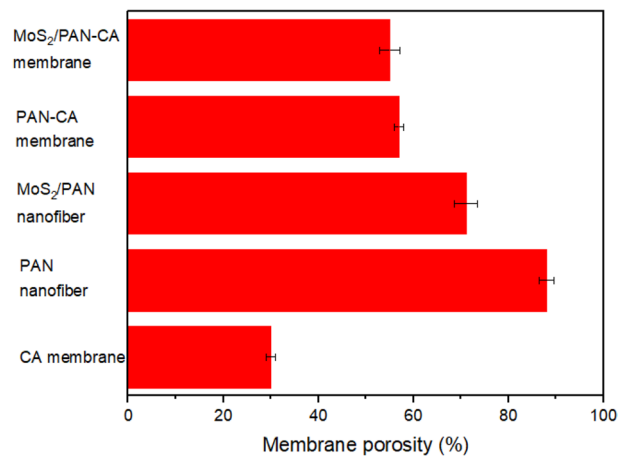

Fig. 10 Membrane porosity (%) of the fabricated membranes

pore size of MoS_2/PAN nanofibers facilitates higher adsorption of various contaminants in water sources [52]. Therefore, MoS_2/PAN-CA membrane can be regarded as a highly potential photocatalytic adsorbent that can efficiently remove pollutants from the contaminated water source.

Tensile test measurement

A tensile test was conducted to evaluate the tensile strength of the prepared MoS_2/PAN-CA and pristine CA membranes. ASTM 882 standard was used to determine the tensile strength of the CA membrane and MoS_2/PAN-CA membrane. Meanwhile, ASTM D638 was used for MoS_2/PAN nanofiber samples. Tensile strength is one of the important mechanical properties to ensure the robustness of the membranes. Based on Fig. 11, it was observed that the tensile strength of the pristine CA membrane is higher (23.9 MPa) as compared to the MoS_2/PAN nanofiber (5.0 MPa), and this result is consistent with previously reported studies on CA membrane [31] and PAN nanofibers [53]. However, when hot-pressed was applied, the tensile strength was enhanced by approximately 32.10 MPa for MoS_2/PAN-CA membrane. The improvement was due to the successful coating of MoS_2/PAN nanofiber and its strong attachment to the surface of the CA membrane. On top of that, the hot-pressed treatment applied had caused the structure of this dual-layers membrane to become more compact and have stronger attachment in between layers. These findings align with a previous study that reported the tensile strength and yield stress of nanofiber membranes with hot-pressed treatment improved by 203% and 313% compared to pristine nanofibers samples [54]. In addition, the photograph images shown in Fig. 11 demonstrated that MoS_2/PAN-CA membrane could retain a firm structure and mechanical stability in both dry and wet conditions compared to MoS_2/PAN nanofiber. (Fig. 12).

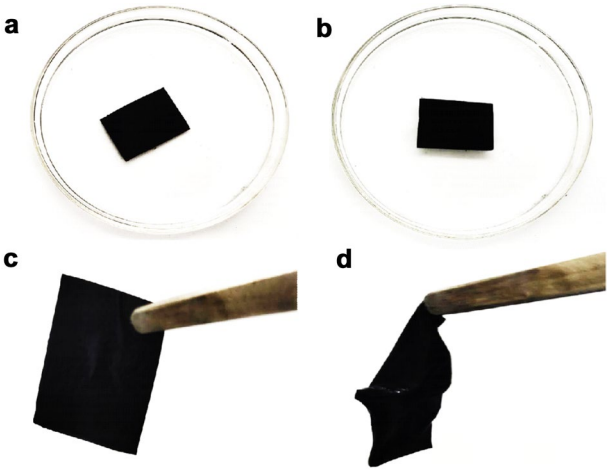

Fig. 12 Photographs images of (**a**) dry MoS_2/PAN nanofiber, (**b**) dry MoS_2/PAN-CA membrane, (**c**) wet MoS_2/PAN nanofiber and (**d**) dry MoS_2/PAN-CA membrane

Pure water flux measurement

The pure water flux measurement was conducted to evaluate the performance of the fabricated CA and MoS_2/PAN-CA membranes in terms of pure water flux. As shown in Fig. 13, the pure water flux of CA membranes was obtained at 36.31 Lm^{-2} $h.^{-1}$, which increased 28% upon coating with MoS_2/PAN nanofibers. This is possibly due to the uniform nanofiber and porous structure of the MoS_2/PAN nanofiber that enhanced the water permeation through the membrane [37, 55, 56]. On top of that, the unique layer structure of MoS_2 with the S chemical component exposed on the membrane surface provides a high number of active sites for strong affinity with water molecules. Besides that, the porous structure of nanofiber coating enhances the adsorption, thus

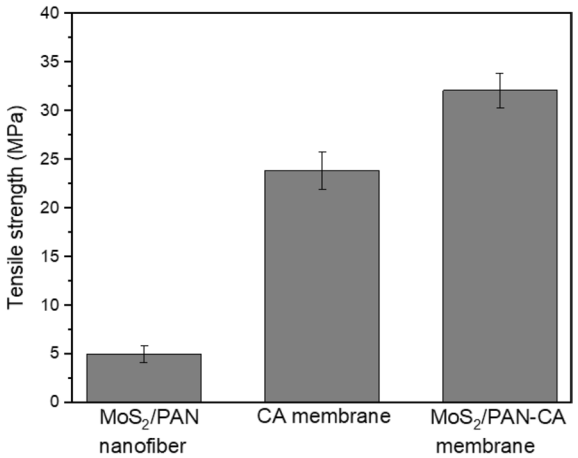

Fig. 11 Analysis of tensile test on CA membrane and MoS_2/PAN-CA membrane

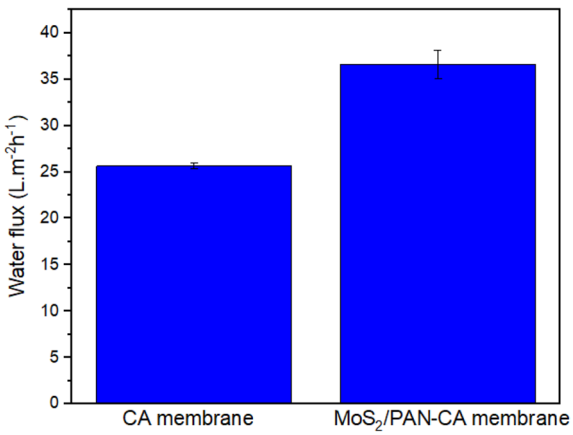

Fig. 13 Water flux analysis on CA membrane and MoS_2/PAN-CA membrane

becoming the contributing factor to the enhancement of pure water flux. On the contrary, the hot-pressed treatment on the CA membrane has changed its structure to become denser, which plausibly caused the lower pure water flux of CA membranes compared to MoS_2/PAN-CA membranes. This denser structure of the membrane also owned a smaller mean pore size and lowered pure water flux [55, 56]

Conclusion

MoS_2/PAN-CA membranes were successfully fabricated by coating the electrospun MoS_2/PAN nanofiber onto flat sheet CA membranes. Besides that, hot-pressed treatment was also applied to enhance the attachment of the MoS_2/PAN on the membrane substrate. The SEM images of the MoS_2/PAN-CA membrane displayed a straight, uniform nanofiber diameter and excellent distribution of exfoliated MoS_2 in the PAN nanofiber, which is favourable to improving the surface structure of CA membranes which own macrovoids. On top of that, hot-pressed treatment at the temperature of 120 °C has also resulted in MoS_2/PAN-CA membrane improving the morphological structure with a strong attachment of both nanofiber layers and CA membrane support. The tensile test confirms the improved mechanical strength of the MoS_2/PAN-CA membrane that demonstrated 32.1 MPa tensile strength, which doubled the strength of the CA membrane. MoS_2/PAN nanofiber coating on the CA membrane facilitates the higher pure water of the membrane due to the uniform and porous nanofiber structure and high affinity of MoS_2 towards the adsorption of water molecules. The pure water flux has increased up to 28% upon coating MoS_2/PAN nanofiber on the membrane. These improved properties of dual-layered adsorptive-photocatalytic MoS_2/PAN-CA membrane recommend it as a potential membrane material to treat various pollutants in water and wastewater.

Acknowledgements The authors were gratefully acknowledged by the Malaysia Ministry of Higher Education (MOHE) for the FRGS research funding (600-IRMI/FRGS 5/3 (441/2019). In addition, NSJ would like to thank Advanced Membrane Technology Research Centre (AMTEC), Universiti Teknologi Malaysia (UTM), Malaysia, for the awarded AMTEC fellowship program.

Author Contributions NSJ as the main author who performed the experiment and wrote the manuscript, NHA and JJ supervised all the laboratory work, and WJL provided the sample & context. At the same time, NHO, FM, SS and MHAA co-wrote the discussion section. All authors read and approved the final manuscript.

Funding Our utmost appreciation to the Malaysia Ministry of Higher Education (MOHE) for the FRGS research funding (600-IRMI/FRGS 5/3 (441/2019).

Data Availability Not applicable.

Declarations

Competing interests The authors declare the following financial interests/personal relationships, which may be considered as potential competing interests by the Malaysia Ministry of Higher Education (MOHE) for the FRGS research funding (600-IRMI/FRGS 5/3 (441/2019).

Ethical Approval Not applicable.

Consent to Publish All authors consent to publish in this journal.

Consent to Participate All authors consent to participate.

References

1. Lu F, Astruc D (2020) Nanocatalysts and other nanomaterials for water remediation from organic pollutants. Coord Chem Rev 408:213180. https://doi.org/10.1016/J.CCR.2020.213180
2. Alias NH, Jaafar J, Samitsu S, Ismail AF, Othman MHD, Rahman MA, Othman NH, Yusof N, Aziz F, Mohd TAT (2020) Efficient removal of partially hydrolysed polyacrylamide in polymer-flooding produced water using photocatalytic graphitic carbon nitride nanofibres. Arab J Chem 13(2):4341–4349. https://doi.org/10.1016/j.arabjc.2019.08.004
3. Sutar RS, Barkul RP, Patil MK (2021) Sunlight assisted photocatalytic degradation of different organic pollutants and simultaneous degradation of cationic and anionic dyes using titanium and zinc based nanocomposites. J Mol Liq. https://doi.org/10.1016/J.MOLLIQ.2021.117191
4. Hashimah N, Jaafar J, Samitsu S, Ismail AF, Nor NAM, Yusof N, Aziz F (2020) Mechanistic insight of the formation of visible-light responsive nanosheet graphitic carbon nitride embedded polyacrylonitrile nanofibres for wastewater treatment. J Water Process Eng. https://doi.org/10.1016/j.jwpe.2019.101015
5. Almasian A, Giahi M, Fard GC, Dehdast SA, Maleknia L (2018) Removal of heavy metal ions by modified PAN/PANI-nylon core-shell nanofibers membrane: filtration performance, antifouling and regeneration behavior. Chem Eng J 351:1166–1178. https://doi.org/10.1016/j.cej.2018.06.127
6. Liu G, Han K, Zhou Y, Ye H, Zhang X, Hu J, Li X (2018) Facile synthesis of highly dispersed ag doped graphene oxide/titanate nanotubes as a visible light photocatalytic membrane for water treatment. ACS Sustain Chem Eng 6:6256–6263. https://doi.org/10.1021/ACSSUSCHEMENG.8B00029
7. Abdullah N, Yusof N, Lau WJ, Jaafar J, Ismail AF (2019) Recent trends of heavy metal removal from water/wastewater by membrane technologies. J Ind Eng Chem 76:17–38
8. Boopathy G, Gangasalam A, Mahalingam A (2020) Photocatalytic removal of organic pollutants and self-cleaning performance of PES membrane incorporated sulfonated graphene oxide/ZnO nanocomposite. J Chem Technol Biotechnol 95:3012–3023. https://doi.org/10.1002/JCTB.6462
9. Lee H, Kim IS (2018) Nanofibers: emerging progress on fabrication using mechanical force and recent applications. Polym Rev 58:688–716. https://doi.org/10.1080/15583724.2018.1495650
10. Fan JP, Luo JJ, Zhang XH, Zhen B, Dong CY, Li YC, Shen J, Cheng YT, Chen HP (2019) A novel electrospun B-CD/CS/PVA nanofiber membrane for simultaneous and rapid removal of organic micropollutants and heavy metal ions from water. Chem Eng J 378:122232. https://doi.org/10.1016/j.cej.2019.122232
11. Nasir AM, Awang N, Jaafar J, Ismail AF, Othman MHD, Rahman MA, Aziz F, Mat Yajid MA (2021) Recent progress on fabrication and application of electrospun nanofibrous photocatalytic

membranes for wastewater treatment: A review. J Water Process Eng. https://doi.org/10.1016/j.jwpe.2020.101878
12. Tijing LD, Yao M, Ren J, Park C (2019) Nanofibers for water and wastewater treatment : recent advances and developments. In: Bui X-T, Chiemchaisri C, Fujioka T, Varjani S (eds) Water and Wastewater Treatment Technologies. Springer, Singapore
13. Deng S, Liu X, Liao J, Lin H, Liu F (2019) PEI modified multiwalled carbon nanotube as a novel additive in PAN nanofiber membrane for enhanced removal of heavy metal ions. Chem Eng J. https://doi.org/10.1016/j.cej.2019.122086
14. Romay M, Diban N, Rivero MJ, Urtiaga A, Ortiz I (2020) Critical issues and guidelines to improve the performance of photocatalytic polymeric membranes. Catalysts 10:570. https://doi.org/10.3390/catal10050570
15. Cao W, Zhang Y, Shi Z, Liu T, Song X, Zhang L, Keung Wong P, Chen Z (2020) Boosting the adsorption and photocatalytic activity of carbon fiber/MoS_2-based weavable photocatalyst by decorating UiO-66-NH_2 nanoparticles. Chem Eng J. https://doi.org/10.1016/j.cej.2020.128112
16. Liu C, Jia F, Wang Q, Yang B, Song S (2017) Two-dimensional molybdenum disulfide as adsorbent for high-efficient Pb(II) removal from water. Appl Mater Today 9:220–228. https://doi.org/10.1016/j.apmt.2017.07.009
17. Jia F, Sun K, Yang B, Zhang X, Wang Q, Song S (2018) Defect-rich molybdenum disulfide as electrode for enhanced capacitive deionization from water. Desalination 446:21–30. https://doi.org/10.1016/j.desal.2018.08.024
18. Zhang X, Fu K, Su Z (2021) Fabrication of 3D MoS_2-TiO_2@PAN electro-spun membrane for efficient and recyclable photocatalytic degradation of organic dyes. Mater Sci Eng B. https://doi.org/10.1016/j.mseb.2021.115179
19. Chen Y-C, Lu A-Y, Lu P, Yang X, Jiang C-M, Mariano M, Kaehr B, Lin O, Taylor A, Sharp ID, Li L-J, Chou SS, Tung V (2017) Structurally deformed MoS_2 for electrochemically stable, thermally resistant, and highly efficient hydrogen evolution reaction. Adv Mater 29:1703863. https://doi.org/10.1002/adma.201703863
20. Li X, Peng K (2018) Hydrothermal synthesis of MoS_2 nanosheet/palygorskite nanofiber hybrid nanostructures for enhanced catalytic activity. Appl Clay Sci 162:175–181. https://doi.org/10.1016/j.clay.2018.06.015
21. Zhao H, Liu G, Zhang M, Liu H, Zhang M, Zhou L, Gao J, Jiang Y (2021) Bioinspired modification of molybdenum disulfide nanosheets to prepare a loose nanofiltration membrane for wastewater treatment. J Water Process Eng. https://doi.org/10.1016/J.JWPE.2020.101759
22. Zhou J, Qin Z, Liu T, Ma Y, An Q, Guo H (2019) Fabrication of MoS_2/polyelectrolyte composite membrane on ceramic tube with enhanced nanofiltration performance. Desalin Water Treat 156:46–51. https://doi.org/10.5004/DWT.2019.24256
23. Schneider R, Facure MHM, Alvarenga AD, Chagas PAM, dos Santos DM, Correa DS (2021) Dye adsorption capacity of MoS_2 nanoflakes immobilized on poly(lactic acid) fibrous membranes. ACS Appl Nano Mater 4:4881–4894. https://doi.org/10.1021/ACSANM.1C00442
24. Lu Y, Fang Y, Xiao X, Qi S, Huan C, Zhan Y, Cheng H, Xu G (2018) Petal-like molybdenum disulfide loaded nanofibers membrane with superhydrophilic property for dye adsorption. Coll Surf A Physicochem Eng Asp 553:210–217. https://doi.org/10.1016/J.COLSURFA.2018.05.056
25. Fang LJ, Chen JH, Wang JM, Lin WW, Lin XG, Lin QJ, He Y (2021) Hydrophobic two-dimensional MoS_2 nanosheets embedded in a polyether copolymer block amide (PEBA) membrane for recovering pyridine from a dilute solution. ACS Omega 6:2675–2685. https://doi.org/10.1021/ACSOMEGA.0C04852
26. Dai R, Han H, Wang T, Li X, Wang Z (2021) Enhanced removal of hydrophobic endocrine disrupting compounds from wastewater by nanofiltration membranes intercalated with hydrophilic MoS_2 nanosheets: role of surface properties and internal nanochannels. J Memb Sci. https://doi.org/10.1016/J.MEMSCI.2021.119267
27. Mukherjee R, Bhunia P, De S (2016) Impact of graphene oxide on removal of heavy metals using mixed matrix membrane. Chem Eng J 292:284–297. https://doi.org/10.1016/j.cej.2016.02.015
28. Gokulakrishnan SA, Arthanareeswaran G, László Z, Veréb G, Kertész S, Kweon J (2021) Recent development of photocatalytic nanomaterials in mixed matrix membrane for emerging pollutants and fouling control, membrane cleaning process. Chemosphere. https://doi.org/10.1016/J.CHEMOSPHERE.2021.130891
29. Nascimben Santos E, Ágoston Á, Kertész S, Hodúr C, László Z, Pap Z, Kása Z, Alapi T, Krishnan SAG, Arthanareeswaran G, Hernadi K, Veréb G (2020) Investigation of the applicability of TiO_2, $BiVO_4$, and WO_3 nanomaterials for advanced photocatalytic membranes used for oil-in-water emulsion separation. Asia-Pacific J Chem Eng. https://doi.org/10.1002/APJ.2549
30. Erdmann R, Kabasci S, Heim HP (2021) Thermal properties of plasticized cellulose acetate and its β-relaxation phenomenon. Polymers (Basel). https://doi.org/10.3390/POLYM13091356
31. Ismail N, El-Gendi A, Essawy H, El-Din LN, Abed K, Ahmed A (2019) Impact of graphene/graphene oxide on the mechanical properties of cellulose acetate membrane and promising natural seawater desalination. J Polym Eng 39:794–804. https://doi.org/10.1515/POLYENG-2019-0075
32. Choi HY, Bae JH, Hasegawa Y, An S, Kim IS, Lee H, Kim M (2020) Thiol-functionalized cellulose nanofiber membranes for the effective adsorption of heavy metal ions in water. Carbohydr Polym. https://doi.org/10.1016/j.carbpol.2020.115881
33. Li W, Li T, Li G, An L, Li F, Zhang Z (2017) Electrospun $H_4SiW_{12}O_{40}$/cellulose acetate composite nanofibrous membrane for photocatalytic degradation of tetracycline and methyl orange with different mechanism. Carbohydr Polym 168:153–162. https://doi.org/10.1016/j.carbpol.2017.03.079
34. Krishnan SAG, Abinaya S, Arthanareeswaran G, Govindaraju S, Yun K (2022) Surface-constructing of visible-light Bi_2WO_6/CeO_2 nanophotocatalyst grafted PVDF membrane for degradation of tetracycline and humic acid. J Hazard Mater. https://doi.org/10.1016/J.JHAZMAT.2021.126747
35. Yusof MSM, Othman MHD, Mustafa A, Rahman MA, Jaafar J, Ismail AF (2018) Feasibility study of cadmium adsorption by palm oil fuel ash (POFA)-based low-cost hollow fibre zeolitic membrane. Environ Sci Pollut Res 25:21644–21655. https://doi.org/10.1007/s11356-018-2286-6
36. Nor NAM, Jaafar J, Ismail AF, Mohamed MA, Rahman MA, Othman MHD, Lau WJ, Yusof N (2016) Preparation and performance of PVDF-based nanocomposite membrane consisting of TiO_2 nanofibers for organic pollutant decomposition in wastewater under UV irradiation. Desalination 391:89–97. https://doi.org/10.1016/J.DESAL.2016.01.015
37. Alias NH, Jaafar J, Samitsu S, Matsuura T, Ismail AF, Huda S, Yusof N, Aziz F (2019) Photocatalytic nanofiber-coated alumina hollow fiber membranes for highly efficient oilfield produced water treatment. Chem Eng J 360:1437–1446. https://doi.org/10.1016/j.cej.2018.10.217
38. Zeng H, Yu Z, Shao L, Li X, Zhu M, Liu Y, Feng X, Zhu X (2020) Ag_2CO_3@UiO-66-NH_2 embedding graphene oxide sheets photocatalytic membrane for enhancing the removal performance of Cr(VI) and dyes based on filtration. Desalination. https://doi.org/10.1016/j.desal.2020.114558
39. Feng ZQ, Yuan X, Wang T (2020) Porous polyacrylonitrile/graphene oxide nanofibers designed for high efficient adsorption of chromium ions (VI) in aqueous solution. Chem Eng J. https://doi.org/10.1016/j.cej.2019.123730
40. Rad LR, Momeni A, Ghazani BF, Irani M, Mahmoudi M, Noghreh B (2014) Removal of $Ni2^+$ and $Cd2^+$ ions from aqueous solutions

using electrospun PVA/zeolite nanofibrous adsorbent. Chem Eng J 256:119–127. https://doi.org/10.1016/j.cej.2014.06.066
41. Pandele AM, Comanici FE, Carp CA, Miculescu F, Voicu SI, Thakur VK, Serban BC (2017) Synthesis and characterization of cellulose acetate-hydroxyapatite micro and nano composites membranes for water purification and biomedical applications. Vacuum 146:599–605. https://doi.org/10.1016/j.vacuum.2017.05.008
42. Zhang Y, Zhang H, Li Y, Mao H, Yang G, Wang J (2015) Tuning the performance of composite membranes by optimizing pdms content and cross-linking time for solvent resistant nanofiltration. Ind Eng Chem Res 54:6175–6186. https://doi.org/10.1021/ACS.IECR.5B01236
43. Wu S, Wang J, Jin L, Li Y, Wang Z (2018) Effects of polyacrylonitrile/MoS_2 composite nanofibers on the growth behavior of bone marrow mesenchymal stem cells. ACS Appl Nano Mater 1:337–343. https://doi.org/10.1021/ACSANM.7B00188
44. Benkaddour A, Jradi K, Robert S, Daneault C (2013) Grafting of polycaprolactone on oxidized nanocelluloses by click chemistry. Nanomater. https://doi.org/10.3390/NANO3010141
45. Sudiarti T, Wahyuningrum D, Bundjali B, Made Arcana I (2017) Mechanical strength and ionic conductivity of polymer electrolyte membranes prepared from cellulose acetate-lithium perchlorate. IOP Conf Ser Mater Sci Eng. https://doi.org/10.1088/1757-899X/223/1/012052
46. Maria da Conceição C, Lucena AE, de Alencar V, Mazzeto SE, de Soares AS (2003) The effect of additives on the thermal degradation of cellulose acetate. Polym Degrad Stab 80:149–155. https://doi.org/10.1016/S0141-3910(02)00396-8
47. Tijing LD, Woo YC, Johir MAH, Choi JS, Shon HK (2014) A novel dual-layer bicomponent electrospun nanofibrous membrane for desalination by direct contact membrane distillation. Chem Eng J 256:155–159. https://doi.org/10.1016/j.cej.2014.06.076
48. Alias NH, Jaafar J, Samitsu S, Yusof N, Othman MHD, Rahman MA, Ismail AF, Aziz F, Salleh WNW, Othman NH (2018) Photocatalytic degradation of oilfield produced water using graphitic carbon nitride embedded in electrospun polyacrylonitrile nanofibers. Chemosphere. https://doi.org/10.1016/j.chemosphere.2018.04.033
49. Kumar M, Jaafar J (2018) Preparation and characterization of TiO+ nanofiber coated PVDF membrane for softdrink wastewater treatment. Environ Ecosyst Sci. https://doi.org/10.26480/ees.02.2018.35.38
50. Islam MS, Sultana S, Rahaman MS (2016) Electrospun nylon 6 microfiltration membrane for treatment of brewery wastewater. AIP Conf Proc. https://doi.org/10.1063/1.4958458
51. Wang Z, Sahadevan R, Crandall C, Menkhaus TJ, Fong H (2020) Hot-pressed PAN/PVDF hybrid electrospun nanofiber membranes for ultrafiltration. J Memb Sci. https://doi.org/10.1016/j.memsci.2020.118327
52. Akduman C, Akçakoca Kumbasar EP, Morsunbul S (2017) Electrospun nanofiber membranes for adsorption of dye molecules from textile wastewater. IOP Conf Ser Mater Sci Eng. https://doi.org/10.1088/1757-899X/254/10/102001
53. Shin WK, Yoo JH, Choi W, Chung KY, Jang SS, Kim DW (2015) Cycling performance of lithium-ion polymer cells assembled with a cross-linked composite polymer electrolyte using a fibrous polyacrylonitrile membrane and vinyl-functionalized SiO_2 nanoparticles. J Mater Chem A 3:12163–12170. https://doi.org/10.1039/C5TA01436K
54. Kaur S, Barhate R, Sundarrajan S, Matsuura T, Ramakrishna S (2011) Hot pressing of electrospun membrane composite and its influence on separation performance on thin film composite nanofiltration membrane. Desalination 279:201–209. https://doi.org/10.1016/j.desal.2011.06.009
55. Liu Q, Huang S, Zhang Y, Zhao S (2018) Comparing the antifouling effects of activated carbon and TiO_2 in ultrafiltration membrane development. J Colloid Interface Sci 515:109–118. https://doi.org/10.1016/j.jcis.2018.01.026
56. Ibrahim Y, Naddeo V, Banat F, Hasan SW (2020) Preparation of novel polyvinylidene fluoride (PVDF)-Tin(IV) oxide (SnO_2) ion exchange mixed matrix membranes for the removal of heavy metals from aqueous solutions. Sep Purif Technol 250:117250. https://doi.org/10.1016/j.seppur.2020.117250